Vav Regulates Peptide-specific Apoptosis in Thymocytes

By Young-Yun Kong,*‡§ Klaus-Dieter Fischer,¶ Martin F. Bachmann,** Sanjeev Mariathasan,‡§ Ivona Kozieradzki,*‡§ Mai P. Nghiem,*‡§ Dennis Bouchard,*‡§ Alan Bernstein,‡‡ Pamela S. Ohashi,‡§ and Josef M. Penninger*‡§

*From the *Amgen Institute, ‡Ontario Cancer Institute, §Department of Medical Biophysics and Department of Immunology, and ‖Department of Medical Genetics, University of Toronto, Toronto, Ontario, Canada M5G 2C1; the ¶Institute for Radiation and Cell Research, University of Würzburg, D-97078 Würzburg, Germany; the **Basel Institute for Immunology, CH 4005 Basel, Switzerland; and the ‡‡Samuel Lunenfeld Research Institute, Mount Sinai Hospital, Toronto, Ontario, Canada M5G 1X5*

Summary

The protooncogene Vav functions as a GDP/GTP exchange factor (GEF) for Rho-like small GTPases involved in cytoskeletal reorganization and cytokine production in T cells. Gene-targeted mice lacking Vav have a severe defect in positive and negative selection of T cell antigen receptor transgenic thymocytes in vivo, and $vav^{-/-}$ thymocytes are completely resistant to peptide-specific and anti-CD3/anti-CD28–mediated apoptosis. Vav acts upstream of mitochondrial pore opening and caspase activation. Biochemically, Vav regulates peptide-specific Ca^{2+} mobilization and actin polymerization. Peptide-specific cell death was blocked both by cytochalasin D inhibition of actin polymerization and by inhibition of protein kinase C (PKC). Activation of PKC with phorbol ester restored peptide-specific apoptosis in $vav^{-/-}$ thymocytes. Vav was found to bind constitutively to PKC-θ in thymocytes. Our results indicate that peptide-triggered thymocyte apoptosis is mediated via Vav activation, changes in the actin cytoskeleton, and subsequent activation of a PKC isoform.

Key words: Vav • negative selection • actin cytoskeleton • signaling transduction • protein kinase C

Engagement of the TCR initiates a cascade of molecular events resulting in tyrosine phosphorylation of cytoplasmic proteins, Ca^{2+} mobilization, activation of the mitogen-activated protein kinase (MAPK)[1] and stress-activated protein kinase (SAPK) pathways, and reorganization of the cytoskeleton. The protooncogene product Vav is expressed in hematopoietic cells and is rapidly phosphorylated after activation of T cells by various growth factors or by cross-linking of antigen receptors (1–3). Vav contains a collection of structural motifs, including a pleckstrin homology (PH) domain, known to facilitate membrane localization; a calponin homology (CH) domain, involved in actin binding; one Src homology (SH)2 domain and two SH3 domains, known to mediate protein–protein interactions; and a Dbl homology (DH) domain (1, 4). In the protooncogene Dbl, the DH domain confers the capacity for guanine nucleotide exchange for the Rho family of small GTPases, which regulate cytoskeletal organization and SAPK/JNK signaling (5–10). Although Vav has been implicated in Ras and MAPK signaling (1, 11, 12), recent biochemical and genetic studies have established a role for Vav in the activation of Rac1 and other members of the Rho family of small GTPases (13–15).

T cells from $vav^{-/-}$ mice exhibit a block in cell cycle progression and fail to produce IL-2 in response to anti-CD3 cross-linking (16–18). Although Vav has no apparent role in TCR-mediated signaling pathways leading to MAPK or SAPK activation after CD3ε cross-linking, Vav has been shown to regulate TCR-mediated Ca^{2+} flux and reorganization of the actin cytoskeleton. Consistent with this role, the functional defects observed in $vav^{-/-}$ T cells can be mimicked using the actin polymerization inhibitor cytochalasin D (CytD [19, 20]). In addition, Vav has been found

[1]*Abbreviations used in this paper:* 7-AAD, 7-amino-actinomycin D; β2m, β2-microglobulin; CytD, cytochalasin D; F-actin, filamentous actin; JNK, c-Jun NH_2-terminal kinase; LCMV, lymphocytic choriomeningitis virus; MAPK, mitogen-activated protein kinase; NF-κB, nuclear factor κB; PI3′K, phosphatidylinositol 3′-kinase; PKC, protein kinase C; SAPK, stress-activated protein kinase; Tg, transgenic.

Y.-Y. Kong and K.-D. Fischer contributed equally to this work.

 J. Exp. Med. © The Rockefeller University Press • 0022-1007/98/12/2099/13 $2.00
Volume 188, Number 11, December 7, 1998 2099–2111
http://www.jem.org

to have a crucial role in thymocyte development and positive selection of both MHC class I– and MHC class II–restricted TCR transgenic (Tg) thymocytes (16–18, 21). However, it has been reported that superantigen-reactive and alloreactive *vav*$^{-/-}$ thymocytes could still undergo negative selection (21), suggesting a differential requirement for Vav in positive versus negative thymocyte selection.

To examine the role of Vav in the selection and activation of peptide-specific thymocytes, we introduced the H-Y TCR (22) and the lymphocytic choriomeningitis virus (LCMV) p33 peptide–specific P14 TCR transgenes (23) into a *vav*$^{-/-}$ background. We report that Vav is essential for peptide-specific clonal deletion and TCR-triggered apoptosis. Vav was found to regulate peptide-specific Ca^{2+} mobilization and actin polymerization in thymocytes. Peptide-triggered apoptosis could be blocked using the actin polymerization inhibitor CytD and a global protein kinase C (PKC) blocker. Among all PKC isoforms tested, only PKC-θ was found to associate with Vav in thymocytes. These results suggest that TCR-mediated changes in the actin cytoskeleton and PKC-θ are crucial prerequisites for negative selection and peptide-triggered apoptosis.

Materials and Methods

Mice. Gene-targeted mice made deficient in Vav by homologous recombination (19), and H-Y and P14 TCR Tg, and P14 Tg β_2-microglobulin $(\beta 2m)^{-/-}$ mice have been described previously (22, 24–27). Mice were screened for the TCR transgene using mAbs against the Tg TCRVβ8 chain. The *vav* mutation was identified using genomic Southern blotting and PCR. Care of animals was in accordance with institutional guidelines.

Reagents. The PKC blockers RO-31-8220 (which blocks all PKC isoforms) and GF109023X (which inhibits the activity of only the Ca^{2+}-dependent PKC isoforms PKC-α, -β, and -γ) were purchased from Calbiochem Corp. (La Jolla, CA [28]). The phosphatidylinositol 3′-kinase (PI3′K)-specific inhibitor Wortmannin and the fungal metabolite CytD (which blocks actin polymerization) were obtained from Sigma Chemical Co. (St. Louis, MO). Phalloidin binds specifically to polymerized filamentous actin (F-actin) and was directly labeled with FITC (Sigma Chemical Co.).

Induction of Apoptosis. Freshly isolated thymocytes from C57BL/6 mice were cultured in RPMI 1640 medium containing 10% FCS and 10^{-5} M β-mercaptoethanol in the absence or presence of dexamethasone (Sigma Chemical Co.), anti-CD95 (clone Jo91; PharMingen, San Diego, CA), anti-CD3ε (clone 145-2C11; PharMingen), anti-CD3ε plus anti-CD28 (clone 37.51), or PMA (12.5 ng/ml) plus Ca^{2+} ionophore A23617 (100 ng/ml), for different time periods and at different concentrations as indicated in figure legends. Optimal concentrations and activation regimes for the induction of apoptosis were determined in pilot studies (29, and data not shown).

Immunocytometry. Blood samples (20 μl) were collected in heparinized capillary tubes and washed once in immunofluorescence staining buffer (1% FCS, 0.01% NaN_3 in PBS). Single cell suspensions of thymocytes, spleen cells, and mesenteric lymph node cells were prepared as described (29), resuspended in PBS, and incubated with the appropriate mAbs for 30 min at 4°C. The following mAbs were used: anti-CD4 (FITC- or PE-labeled; PharMingen); anti-CD8 (FITC- or PE-labeled, or biotinylated; Serotec, Inc., Raleigh, NC); anti-pan TCR-α/β (FITC- or PE-labeled; PharMingen); anti-TCRVβ8.1+8.2 (clone KJ16, PE-labeled or biotinylated; PharMingen); anti–H-2K^b (FITC-labeled or biotinylated; PharMingen); anti–H-2K^d (FITC-labeled; PharMingen); anti-CD5 (biotinylated; PharMingen); anti-CD28 (biotinylated; PharMingen); anti-HSA (biotinylated; PharMingen); anti-CD69 (biotinylated; PharMingen); anti-CD3ε (FITC- or PE-labeled; PharMingen); anti–H-Y TCR clonotype (T3.70; FITC-labeled or biotinylated); anti-TCRVβ8 (biotinylated; PharMingen); and anti-P14 TCRVα2 (biotinylated; PharMingen). All staining combinations were as indicated in figure legends. Biotinylated mAbs were visualized with Streptavidin-RED670 (GIBCO BRL, Gaithersburg, MD), and samples were analyzed using a FACScan® and Lysis II software (Becton Dickinson, Mountain View, CA).

Negative Selection In Vitro. Thymocytes were purified from *vav*$^{+/+}$, *vav*$^{+/-}$, and *vav*$^{-/-}$ P14 Tg mice. P14 Tg mice express an α/β TCR (TCRVα2Vβ8) specific for the strong agonist p33 peptide of LCMV. Thymocytes were cultured on EL4 cells (H-2$^{b/b}$) in RPMI medium containing 5% FCS and 10^{-5} M β-mercaptoethanol (2 ml final vol/well of 24-well flat-bottomed plates; Costar Corp., Cambridge, MA). EL4 cells (H-2$^{b/b}$) were pulsed with different concentrations of the deleting p33 peptide or the weak agonist p33 peptide analogue 8.1 for 2 h before coculture with thymocytes (26, 27, 30). Thymocytes were harvested after 10, 16, and 22 h of incubation and stained with anti-CD4–PE, anti-CD8–FITC, and the chromogenic dye 7-amino-actinomycin D (7-AAD; Calbiochem Corp.). 7-AAD is a vital dye that enters dead cells after the loss of membrane integrity and allows quantitation of apoptotic cells by cytometry (FL-3 channel on a FACScan® [31]). Apoptosis was also determined by trypan blue exclusion and by staining with propidium iodide and annexin V (R&D Systems, Inc., Minneapolis, MN). Propidium iodide and annexin V staining of thymocytes was determined by cytofluorometry using a FACScalibur® (Becton Dickinson). Percent survival was calculated as [(total number of viable $CD4^+CD8^+$ thymocytes cultured at different LCMV-peptide concentrations)/(total number of viable $CD4^+CD8^+$ thymocytes from the same mouse cultured with EL4 cells at 37°C in the absence of peptide)] × 100.

Mitochondrial Permeability Transition ($\Delta\Psi_m$ Disruption). The mitochondrial transmembrane potential ($\Delta\Psi_m$) results from the asymmetric distribution of protons across the inner mitochondrial membrane, giving rise to a chemical (pH) and electric gradient (32, 33). The inner side of the inner mitochondrial membrane is negatively charged. As a consequence, the cationic lipophilic fluorochrome 3,3′-dihexyloxacarbocyanine iodide [$DiOC_6(3)$] is distributed on the mitochondrial matrix, correlating with $\Delta\Psi_m$. $DiOC_6(3)$ can be used to measure variations in the $\Delta\Psi_m$ on a per cell basis. Cells induced to undergo apoptosis manifest an early reduction in the incorporation of $\Delta\psi_m$-sensitive dyes, indicating a disruption of $\Delta\psi_m$. For $DiOC_6(3)$ staining, 10^6 thymocytes were incubated with $DiOC_6(3)$ (final concentration 20 nM in PBS) for 20 min at 37°C. $DiOC_6(3)$ staining was analyzed immediately using a FACScan®.

Signal Transduction. Thymocytes were isolated from nonselecting *β2m*$^{-/-}$ *vav*$^{+/+}$, positively selecting *vav*$^{+/-}$, and *vav*$^{-/-}$ P14 Tg mice and cultured on a monolayer of confluent and adherent MC57G fibroblasts (H-2$^{b/b}$) in RPMI medium containing 5% FCS and 10^{-5} M β-mercaptoethanol. MC57G APCs were pulsed with different concentrations of the agonist LCMV–p33 peptide or the control AV peptide for 2 h before coculture with thymocytes. Nonadherent thymocytes (2×10^6 P14 Tg thymocytes/well) were harvested after 15, 30, 60, and 180 min of

coculture with adherent fibroblasts and assayed for MAPK and SAPK activation, nuclear factor κB (NF-κB) activation (IκB phosphorylation), and phosphotyrosine signaling (19). In brief, tyrosine phosphorylation was monitored in total cell lysates and immunoprecipitates using an antiphosphotyrosine mAb (Upstate Biotechnology, Inc., Lake Placid, NY). Activation of SAPKs and MAPKs was detected using phospho-SAPK– and phospho-MAPK–specific Abs (New England Biolabs Inc., Beverly, MA). The levels of SAPK and MAPKs (extracellular signal–regulatory kinase [ERK]1/ERK2) were determined by immunoblotting (New England Biolabs Inc.). Phosphorylated IκB was detected using an mAb specific for phosphoserine (Ser32) of IκBα (New England Biolabs Inc.). Ser32 phosphorylation of IκBα targets IκB for degradation and is essential for the release of active NF-κB (34).

Immunoprecipitation. Thymocytes and peripheral lymph node T cells were activated with anti-CD3ϵ (1 μg/ml) for different time periods as indicated in figure legends. Cells (10^7/lane) were harvested and lysed, and Vav was immunoprecipitated using an anti-Vav1 Ab reactive against amino acids 576–589 (Santa Cruz Biotechnology Inc., Santa Cruz, CA). Immunocomplexes were separated by SDS-PAGE, transferred onto a membrane, and Western blotted to detect the presence of Vav and the PKC isoforms PKC-α, -β (-βI and -βII), -γ, -δ, -ϵ, -ζ, -θ, -ι, -λ, -μ, and receptor for activated C-kinase 1 (RACK1). In parallel, total cell lysates (2×10^6 cells/lane) were Western blotted to ascertain the relative protein levels of these PKC isoforms in thymocytes. All PKC isoform Abs were purchased from Transduction Laboratories (Lexington, KY).

Peptide-specific Ca^{2+} Mobilization. Peptide-specific Ca^{2+} mobilization ($[Ca^{2+}]_i$) in P14 thymocytes was determined as described (35). In brief, freshly isolated P14 Tg thymocytes (2×10^6) were loaded with 3 mM INDO-1 (Molecular Probes, Inc., Eugene, OR) in IMDM (pH 7.4) for 1 h at 37°C. Thymocytes were then incubated with peptide-presenting EL4 cells loaded with either p33 or AV peptide and centrifuged (1,500 rpm, 4°C) to allow conjugate formation between thymocytes and EL4 cells. Increases in intracellular free Ca^{2+} were recorded in real time on live-gated thymocyte–EL4 conjugates using a FACScalibur® (Becton Dickinson).

Actin Polymerization. Thymocytes were preincubated with PMA (12.5 ng/ml), and EL4 cells were loaded with either p33 or AV peptide (10^{-6} M) for 30 min on ice. Actin polymerization was initiated by placing the cells at 37°C for different time periods as indicated in figure legends. Activation was stopped by addition of 4% paraformaldehyde. After fixation, cells were incubated for 30 min with FITC-labeled phalloidin, which specifically binds to polymerized F-actin. Cells were washed three times in PBS, and phalloidin staining was analyzed using a FACScan®. Percentage of peptide-specific actin polymerization (percent F-actin) was calculated as [(mean value of phalloidin fluorescence intensity of p33-activated cells at a certain time point)/(mean value of phalloidin fluorescence intensity of AV-activated cells at the same time point)] × 100.

Results

Impaired TCR-mediated Positive Selection of $vav^{-/-}$ Thymocytes. To analyze the role in vivo of Vav in thymocyte selection, we introduced two rearranged TCR-α/β transgenes, H-Y and P14, into a $vav^{-/-}$ background. The H-Y TCR recognizes a male-specific peptide in the context of MHC class I. Thymocytes expressing the H-Y TCR are positively selected in female H-2^b mice (22, 24, 25). The P14 TCR is specific for a peptide epitope of the LCMV glycoprotein p33 in the context of the MHC haplotype H-$2D^b$ (23). In positively selecting $vav^{+/-}$ mice, the development of $P14^+$ and H-Y^+ thymocytes is skewed towards the $CD8^+$ lineage (Fig. 1, *A* and *B*). In $vav^{-/-}$ mice, this bias in favor of mature $CD8^+$ thymocytes did not occur in either H-Y Tg or P14 Tg thymocytes (Fig. 1, *A* and *B*), and development was in fact blocked at the immature $CD4^+$ $CD8^+$ stage of differentiation. Consistent with a block in positive selection, TCR Tg $vav^{-/-}$ thymocytes expressed high levels of HSA and did not upregulate surface expression of the maturation and selection markers CD69, CD5 (Fig. 1 *C*), H-$2K^b$, or CD45RB (not shown). Expression of the P14 Tg TCRVβ8 and TCRVα2 chains was significantly lower in immature $CD4^+CD8^+$ thymocytes of $vav^{-/-}$ mice compared with $CD4^+CD8^+$ thymocytes from $vav^{+/-}$ mice (Fig. 1 *C*). Similarly, expression of the H-Y Tg–specific TCRVβ8 and TCRVα3 chains detected by the T3.70 Ab was significantly lower in H-Y Tg $vav^{-/-}$ mice (not shown). Importantly, P14 Tg $vav^{-/-}$ (and H-Y Tg $vav^{-/-}$ [not shown]) thymocytes displayed a phenotype that is similar to that of P14 Tg (and H-Y) $vav^{+/+}$ $\beta 2m^{-/-}$ mice, which have a defect in positive selection of MHC class I–restricted thymocytes (Fig. 1 *C*). These results show that Vav regulates the positive selection of MHC class I–restricted thymocytes and confirm previous data demonstrating the crucial role of Vav in positive thymocyte selection (16–18, 21).

Impaired Negative Selection and Peptide-specific Apoptosis. To examine the role of Vav in peptide-specific clonal deletion in vivo and in vitro, we investigated the negative selection of H-Y and LCMV TCR Tg thymocytes. In the H-Y Tg system, thymocytes expressing the H-Y TCR are positively selected in female H-2^b mice but negatively selected in male H-2^b mice. Negative selection in male H-Y Tg mice results in a small thymus due to deletion of $CD4^+CD8^+$ thymocytes (24; Fig. 1 *B*). However, male $vav^{-/-}$ mice contained a large number of $CD4^+CD8^+$ thymocytes, indicating that negative selection of H-Y Tg thymocytes was severely impaired in the absence of Vav.

To further elucidate the requirement for Vav in negative selection, an in vitro model of peptide-specific negative selection was used (30). In the LCMV–p33 peptide system, APCs are loaded with different concentrations of the LCMV glycoprotein strong agonist peptide p33 or the weak agonist p33 peptide analogue 8.1. Although $vav^{+/-}$ P14 Tg thymocytes readily underwent apoptosis in a dose-dependent manner in response to treatment with either the p33 or 8.1 peptide (Fig. 2 *A*), $vav^{-/-}$ P14 Tg thymocytes were completely resistant to peptide-mediated apoptosis, even at very high peptide concentrations (Fig. 2 *B*). Since P14 $vav^{-/-}$ thymocytes are blocked in positive T cell selection, we used $\beta 2m^{-/-}$ $vav^{+/+}$ P14 TCR Tg mice (H-$2^{b/b}$) as an additional control since these mice have a block in the positive selection of the P14 TCR due to deletion of the MHC class I ligand ($\beta 2m^{-/-}$). The kinetics and extent of

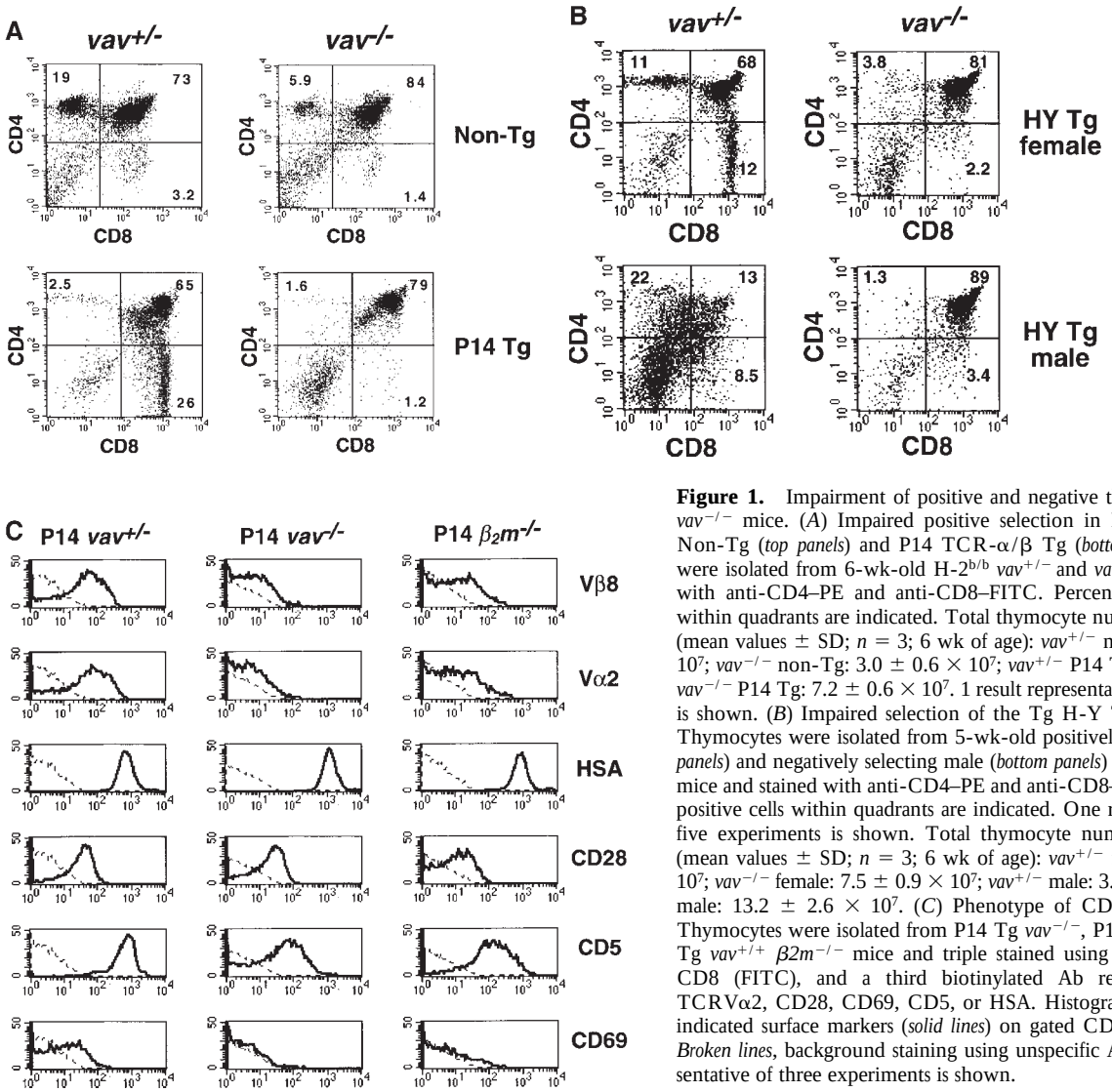

Figure 1. Impairment of positive and negative thymocyte selection in $vav^{-/-}$ mice. (*A*) Impaired positive selection in P14 Tg $vav^{-/-}$ mice. Non-Tg (*top panels*) and P14 TCR-α/β Tg (*bottom panels*) thymocytes were isolated from 6-wk-old H-$2^{b/b}$ $vav^{+/-}$ and $vav^{-/-}$ mice and stained with anti-CD4–PE and anti-CD8–FITC. Percentages of positive cells within quadrants are indicated. Total thymocyte numbers were as follows (mean values ± SD; $n = 3$; 6 wk of age): $vav^{+/-}$ non-Tg: $11.2 \pm 2.5 \times 10^7$; $vav^{-/-}$ non-Tg: $3.0 \pm 0.6 \times 10^7$; $vav^{+/-}$ P14 Tg: $12.0 \pm 3.4 \times 10^7$; $vav^{-/-}$ P14 Tg: $7.2 \pm 0.6 \times 10^7$. 1 result representative of 10 experiments is shown. (*B*) Impaired selection of the Tg H-Y TCR in $vav^{-/-}$ mice. Thymocytes were isolated from 5-wk-old positively selecting female (*top panels*) and negatively selecting male (*bottom panels*) H-$2^{b/b}$ H-Y TCR Tg mice and stained with anti-CD4–PE and anti-CD8–FITC. Percentages of positive cells within quadrants are indicated. One result representative of five experiments is shown. Total thymocyte numbers were as follows (mean values ± SD; $n = 3$; 6 wk of age): $vav^{+/-}$ female: $19.6 \pm 3.3 \times 10^7$; $vav^{-/-}$ female: $7.5 \pm 0.9 \times 10^7$; $vav^{+/-}$ male: $3.6 \pm 0.8 \times 10^7$; $vav^{-/-}$ male: $13.2 \pm 2.6 \times 10^7$. (*C*) Phenotype of $CD4^+CD8^+$ thymocytes. Thymocytes were isolated from P14 Tg $vav^{-/-}$, P14 Tg $vav^{+/-}$, and P14 Tg $vav^{+/+}$ $\beta 2m^{-/-}$ mice and triple stained using anti-CD4 (PE), anti-CD8 (FITC), and a third biotinylated Ab reactive to TCRVβ8, TCRVα2, CD28, CD69, CD5, or HSA. Histograms are shown for the indicated surface markers (*solid lines*) on gated $CD4^+CD8^+$ thymocytes. *Broken lines*, background staining using unspecific Abs. One result representative of three experiments is shown.

p33-induced apoptosis of $\beta 2m^{-/-}$ $CD4^+CD8^+$ P14 Tg thymocytes were similar to those of $vav^{+/-}$ P14 Tg mice, indicating that the defect of P14 Tg $vav^{-/-}$ thymocytes to undergo peptide-specific apoptosis was not due to differences in the composition of thymocyte populations (Fig. 2 *C*). These results show that Vav is required for the negative selection of peptide-specific thymocytes.

$vav^{-/-}$ Thymocytes Are Resistant to CD3/CD28-mediated Apoptosis. Immature $CD4^+CD8^+$ thymocytes are highly susceptible to cell death induced by many apoptotic stimuli (36). We evaluated the ability of $vav^{+/-}$ and $vav^{-/-}$ thymocytes to undergo apoptosis in response to the following stimuli: dexamethasone, PMA/Ca^{2+} ionophore, anti-CD95 (FAS), anti-CD3ε, and anti-CD3ε/anti-CD28 (29, 37). Although treatment with anti-CD3ε/anti-CD28 induced the cell death of $vav^{+/-}$ $CD4^+CD8^+$ thymocytes, $vav^{-/-}$ thymocytes were strikingly resistant to anti-CD3ε/anti-CD28–triggered apoptosis (Fig. 3). No significant differences were observed between $vav^{-/-}$, $vav^{+/-}$, and $vav^{+/+}$ thymocytes in the extent or kinetics of cell death in response to anti-CD95 (FAS), PMA plus Ca^{2+} ionophore (Fig. 3), or dexamethasone (not shown), implying that the cellular apoptotic machinery is functional in the absence of Vav. These data indicate that Vav is a crucial signal transduction molecule involved in TCR-mediated thymocyte apoptosis.

Vav Links TCR Signaling to Mitochondrial ($\Delta\psi_m$) Disruption. Disruption of the mitochondrial transmembrane potential ($\Delta\psi_m$) due to the opening of mitochondrial membrane pore complex has been identified as the earliest common denominator of apoptosis (36). Alterations in mitochondria lead to the release of "apoptosis-inducing factor" (AIF) or cytochrome *c*, resulting in the activation of effector caspases such as caspase 3 (Cpp32) (32, 38–41). To assess whether Vav links TCR signaling to the opening of mitochondrial pores, we determined the mitochondrial transmembrane potential

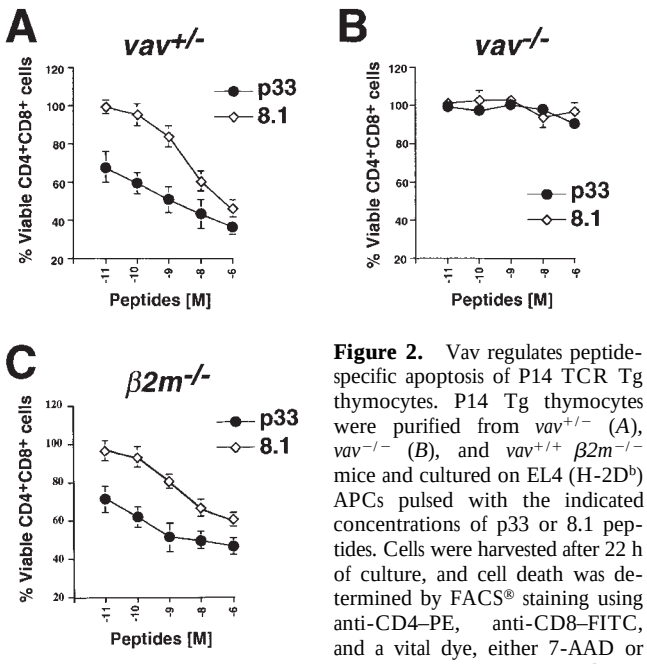

Figure 2. Vav regulates peptide-specific apoptosis of P14 TCR Tg thymocytes. P14 Tg thymocytes were purified from *vav*$^{+/-}$ (*A*), *vav*$^{-/-}$ (*B*), and *vav*$^{+/+}$ *β2m*$^{-/-}$ mice and cultured on EL4 (H-2D^{b}) APCs pulsed with the indicated concentrations of p33 or 8.1 peptides. Cells were harvested after 22 h of culture, and cell death was determined by FACS® staining using anti-CD4–PE, anti-CD8–FITC, and a vital dye, either 7-AAD or annexin V. Percent survival was determined from the number of viable CD4^{+}CD8^{+} thymocytes remaining after culture in a given concentration of p33 or 8.1 peptide compared with the number of control thymocytes remaining after culture in an equal concentration of the control peptide AV. The AV peptide has high affinity for H-2D^{b} but very low affinity for the P14 TCR. Peptide concentrations on the x-axis indicate a range of 10^{-6} to 10^{-11} M. One result representative of five experiments is shown.

($\Delta\psi_m$) by cytometry using the fluorochromic dye $DiOC_6(3)$ (33). Stimulation of P14 Tg *vav*$^{+/-}$ thymocytes with 10^{-6} M p33 peptide led to measurable changes in $\Delta\psi_m$ compared with P14 Tg *vav*$^{+/-}$ thymocytes treated with similar concentrations of the nondeleting control AV peptide (compare Fig. 4, *A* and *C*). However, p33 peptide–triggered disruption of $\Delta\psi_m$ did not occur in *vav*$^{-/-}$ thymocytes (compare Fig. 4, *B* and *D*). Fig. 4 *E* shows that this effect was dose dependent only in P14 Tg *vav*$^{+/-}$ thymocytes. Moreover, peptide-specific activation of the downstream effector caspase 3 (42) did not occur in P14 Tg *vav*$^{-/-}$ thymocytes even when very high concentrations of the deleting p33 peptide were used (not shown). Disruption of $\Delta\psi_m$ and caspase 3 activation occurred normally in *vav*$^{-/-}$ thymocytes treated with dexamethasone or CD95 (not shown).

Vav Regulates Peptide-specific Ca^{2+} Flux and Actin Polymerization. We (19) and other groups (17, 20, 21) have used anti-CD3 cross-linking to establish that Vav links TCR/CD3 activation to the actin cytoskeleton and Ca^{2+} flux. However, these experiments showed that Vav had no apparent role in phosphotyrosine signaling, or in the activation of MAPK, SAPK, or NF-κB. However, the role of Vav in peptide–MHC-mediated physiological responses and peptide–MHC-specific signaling remained obscure. To determine the biochemical defect in *vav*$^{-/-}$ T cells, we analyzed peptide-triggered signaling pathways in P14 TCR Tg thymocytes from *vav*$^{+/+}$, *vav*$^{-/-}$, and various control

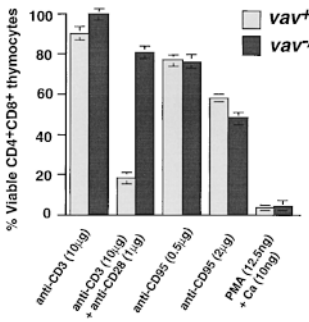

Figure 3. *vav*$^{-/-}$ thymocytes are resistant to anti-CD3/anti-CD28–mediated apoptosis. Cell death was induced in *vav*$^{+/-}$ and *vav*$^{-/-}$ thymocytes by treatment with anti-CD3ε, anti-CD3ε plus anti-CD28, anti-CD95 (FAS), or PMA plus Ca^{2+} ionophore. Percentage of viable CD4^{+}CD8^{+} thymocytes remaining after treatment is indicated on the y-axis. The mean result of a triplicate culture (±SD) representative of three independent experiments is shown for each activation.

strains. Since P14 *vav*$^{-/-}$ thymocytes are blocked in positive T cell selection, we used *β2m*$^{-/-}$ *vav*$^{+/+}$ P14 TCR Tg mice (H-2$^{b/b}$) as an additional control. These mice have a block in the positive selection of the P14 TCR due to the deletion of the MHC class I ligand (*β2m*$^{-/-}$ [27, 43]). The use of *β2m*$^{-/-}$ *vav*$^{+/+}$ P14 Tg mice ensured that thymocytes expressing the Tg TCR chain had not been previously activated by the selecting MHC ligand. TCR levels and expression of maturation markers were similar on the thymocytes of P14 *vav*$^{-/-}$ and P14 *β2m*$^{-/-}$ *vav*$^{+/+}$ mice (Fig. 1 *C*).

P14 *vav*$^{-/-}$, P14 *vav*$^{+/-}$, and P14 *β2m*$^{-/-}$ *vav*$^{+/+}$ thymocytes were cultured with the deleting p33 peptide or the nondeleting control AV peptide for different time periods. No apparent differences were observed between *vav*$^{-/-}$, *vav*$^{+/-}$, and *β2m*$^{-/-}$ *vav*$^{+/+}$ P14 Tg thymocytes in either the extent or kinetics of phosphotyrosine signaling, MAPK activation, or NF-κB activation after p33 peptide–specific activation (not shown). Intriguingly, p33 peptide–MHC-mediated activation of either *vav*$^{-/-}$, *vav*$^{+/-}$, or *β2m*$^{-/-}$ *vav*$^{+/+}$ P14 Tg thymocytes did not lead to any detectable SAPK/JNK activity (not shown). However, p33 peptide–specific Ca^{2+} mobilization was significantly decreased in *vav*$^{-/-}$ P14 thymocytes compared with P14 *β2m*$^{-/-}$ *vav*$^{+/+}$ thymocytes (compare Fig. 5, *C* and *D*) and P14 *vav*$^{+/-}$ thymocytes (not shown). Moreover, phalloidin staining experiments showed that *vav*$^{-/-}$ thymocytes exhibited a decrease in actin polymerization and the formation of F-actin after activation with the deleting p33 peptide (Fig. 6). Peptide–MHC-triggered Ca^{2+} mobilization and actin polymerization were comparable between P14 *vav*$^{+/-}$ and P14 *β2m*$^{-/-}$ *vav*$^{+/+}$ thymocytes (not shown). These results provide the first genetic evidence that Vav links peptide-specific activation of the TCR to cytoskeletal reorganization and Ca^{2+} mobilization.

Treatment with the actin polymerization blocker CytD is known to mimic the functional and biochemical defects observed in peripheral *vav*$^{-/-}$ T cells after CD3 cross-linking (20). It has also been reported that CytD addition impairs peptide-induced Ca^{2+} flux in human CD4^{+} T cell clones (35). Therefore, we analyzed whether CytD treatment could abrogate Ca^{2+} mobilization in freshly isolated, wild-type P14 thymocytes. Incubation of P14 thymocytes

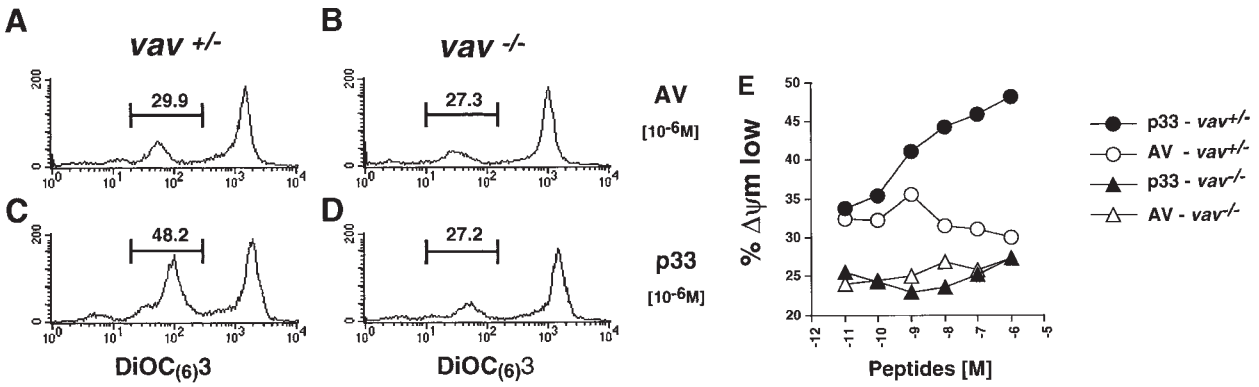

Figure 4. Vav acts upstream of the mitochondrial permeability transition ($\Delta\psi_m$ disruption). (*A–D*) Disruption of $\Delta\psi_m$ was determined by a reduction in the fluorescence intensity of the mitochondrial matrix chromogen $DiOC_6(3)$. Representative histograms of the changes in mitochondrial $DiOC_6(3)$ fluorescence intensity are shown for thymocytes of $vav^{+/-}$ (*A* and *C*) and $vav^{-/-}$ (*B* and *D*) mice treated with the control AV peptide (*A* and *B*) and the deleting p33 peptide (*C* and *D*). EL4 APCs were loaded with 10^{-6} M AV or p33 peptide, washed, and subsequently cultured with $vav^{+/-}$ and $vav^{-/-}$ thymocytes for 16 h. One result representative of three independent experiments is shown. (*E*) Dose–response curve of $\Delta\psi_m$ disruption. Percent change in $\Delta\psi_m$ intensity in $vav^{+/-}$ and $vav^{-/-}$ thymocytes treated with different concentrations of deleting p33 peptide or control AV peptide is shown. EL4 APCs were loaded with the indicated concentration of AV or p33 peptide, washed, and subsequently cultured with $vav^{+/-}$ and $vav^{-/-}$ thymocytes for 10 h. One result representative of three independent experiments is shown.

with CytD (Fig. 5 *E*) or chelation of extracellular Ca^{2+} by EGTA (Fig. 5 *F*) significantly decreased p33 peptide–triggered Ca^{2+} mobilization. The extent of the CytD-mediated decrease in peptide-specific Ca^{2+} flux was dependent on the concentration of the p33 peptide (not shown). Treatment of P14 thymocytes with CytD had no apparent effect on the extent of tyrosine phosphorylation, NF-κB activation, or MAPK activation (not shown). These results

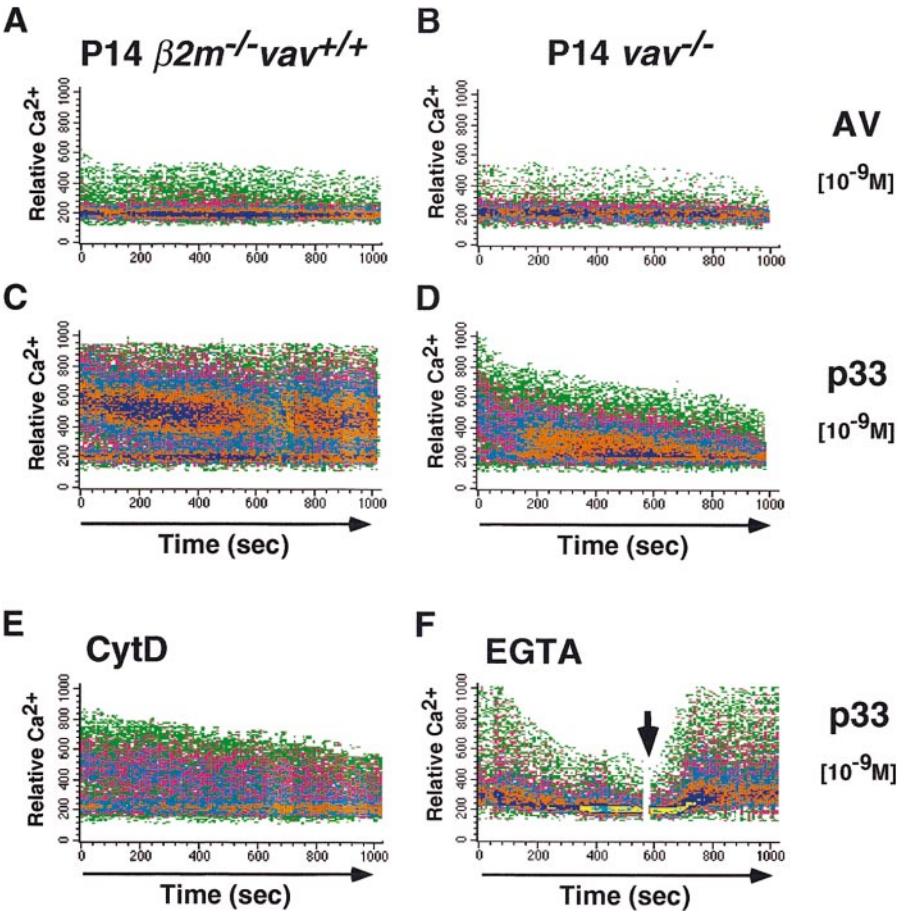

Figure 5. Vav is required for peptide-specific Ca^{2+} mobilization. (*A–D*) Ca^{2+} flux in freshly isolated P14 thymocytes from $\beta2m^{-/-}vav^{+/+}$ (*A* and *C*) and $vav^{-/-}$ (*B* and *D*) mice. X-axis: real time Ca^{2+} release in seconds; y-axis: intensity of increase of intracellular Ca^{2+} in P14 thymocytes after incubation with EL4 APCs loaded with 10^{-9} M AV (*A* and *B*) or p33 (*C* and *D*) peptide. The Ca^{2+} flux in $\beta2m^{-/-}vav^{+/+}$ P14 thymocytes was similar in intensity and kinetics to that in $vav^{+/+}$ or $vav^{+/-}$ P14 thymocytes (not shown). Similar results were obtained in $vav^{+/-}$ and $vav^{-/-}$ P14 thymocytes using higher concentrations (10^{-8}, 10^{-7}, 10^{-6}, and 10^{-5} M) of p33 and AV peptides (not shown), meaning that higher peptide concentrations did not significantly increase the Ca^{2+} responses detected in $\beta2m^{-/-}vav^{+/+}$, $vav^{+/-}$, or $vav^{-/-}$ P14 thymocytes. One experiment representative of four independent experiments is shown. (*E* and *F*) Effect of CytD and EGTA on Ca^{2+} flux in freshly isolated $\beta2m^{-/-}vav^{+/+}$ P14 thymocytes. Ca^{2+} flux was decreased when p33-loaded (10^{-9} M) EL4 APCs were pretreated 15 min before activation with CytD (*E*). A similar decrease occurred when EGTA (2.5 μM) was added to the cells to block flux by transmembrane Ca^{2+} channels (*F*). As a control for loading, addition of $CaCl_2$ into the medium (*F*, *arrow*) restored Ca^{2+} flux in EGTA-treated cells.

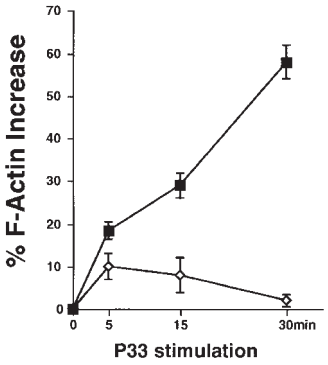

Figure 6. Impaired peptide-specific actin polymerization (F-actin formation) in P14 $vav^{-/-}$ thymocytes. Thymocytes from P14 $vav^{-/-}$ (*diamonds*) and $vav^{+/-}$ (*squares*) littermates were isolated and activated with EL4 APCs loaded with the deleting p33 peptide (10^{-6} M) or the control AV peptide (10^{-6} M) for the indicated time periods. Percentage of actin polymerization (mean percent increase in F-actin ± SD) is shown on the y-axis. Values were calculated as described in Materials and Methods. The x-axis shows the kinetics of induction in minutes after p33 stimulation. One result representative of three independent experiments is shown.

suggest that peptide-specific actin polymerization has an important role in the extent and duration of TCR-mediated Ca^{2+} mobilization in thymocytes.

Inhibition of Actin Polymerization Blocks Peptide-specific Thymocyte Apoptosis. To further elucidate the role of Vav-regulated changes in the actin cytoskeleton during negative selection, we tested whether the actin polymerization inhibitor CytD could interfere with peptide-specific apoptosis of P14 TCR Tg thymocytes. Interestingly, CytD blocked the peptide-specific cell death of $vav^{+/+}$ P14 thymocytes in a dose-dependent manner (Fig. 7). Similarly, anti-CD3/anti-CD28–mediated, but not dexamethasone- or CD95-mediated, apoptosis of $vav^{+/+}$ thymocytes could be inhibited by CytD (not shown). These data suggest that TCR-mediated actin polymerization plays a role in peptide-specific apoptosis of thymocytes.

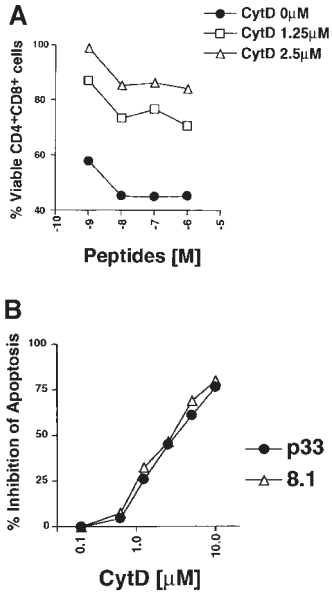

Figure 7. Inhibition of actin polymerization blocks peptide-specific thymocyte apoptosis. (*A*) The actin polymerization inhibitor CytD blocks peptide-specific apoptosis of P14 TCR Tg $vav^{+/+}$ thymocytes induced by different concentrations of the high-affinity p33 peptide. The percentage of viable $CD4^+CD8^+$ cells remaining after treatment is shown on the y-axis. Peptide concentrations are indicated on the x-axis and range from 10^{-6} to 10^{-9} M. The concentrations of CytD used to inhibit thymocyte apoptosis are indicated. (*B*) Dose–response curve of CytD inhibition of peptide-specific apoptosis of P14 Tg $vav^{+/+}$ thymocytes. Percent inhibition of apoptosis is shown on the y-axis. The concentration of the deleting p33 or control AV peptide was 10^{-9} M. Apoptosis of $CD4^+CD8^+$ thymocytes was detected as described in Materials and Methods. One result representative of six experiments is shown.

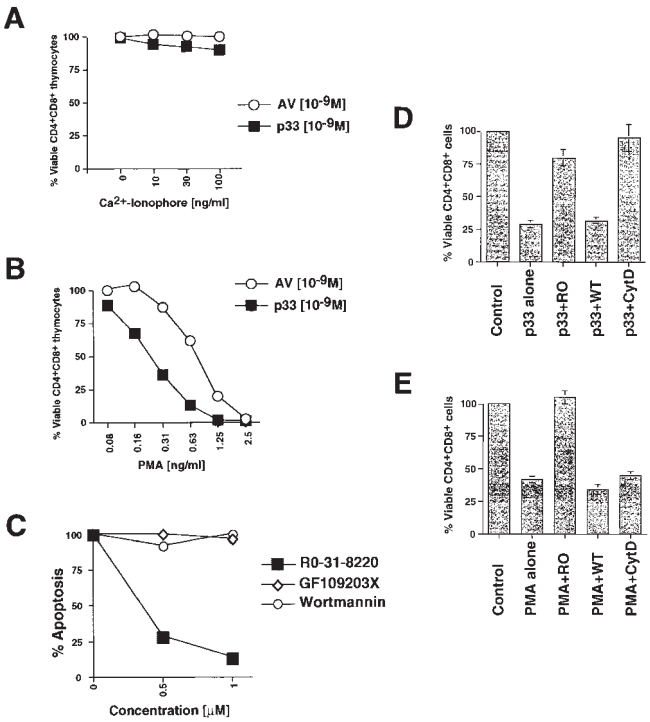

Figure 8. PKC activation can restore peptide-specific apoptosis of P14 $vav^{-/-}$ thymocytes. (*A* and *B*) The specific PKC activator PMA, but not Ca^{2+} ionophore, can rescue peptide-specific apoptosis of $vav^{-/-}$ thymocytes. P14 $vav^{-/-}$ thymocytes (2×10^6/well) were incubated with EL4 APCs loaded with 10^{-9} M AV or p33 peptide plus varying concentrations of the Ca^{2+} ionophore A23617 (*A*) or PMA (*B*). Higher concentrations of the Ca^{2+} ionophore A23617 plus p33 peptide also failed to trigger apoptosis (not shown). Viability of $CD4^+CD8^+$ thymocytes was assessed 16 h after activation as described in Materials and Methods. It should be noted that PMA alone induced apoptosis of $CD4^+CD8^+$ $vav^{-/-}$ thymocytes (not shown). One result representative of three independent experiments is shown. (*C*) Inhibition of p33 peptide–mediated apoptosis of P14 TCR Tg $vav^{+/+}$ thymocytes by the global PKC inhibitor RO-31-8220. Apoptosis was induced by treatment with 10^{-9} M p33 peptide in the presence of the global PKC blocker RO-31-8220, GF109203X (which only inhibits the activity of the Ca^{2+}-dependent PKC-α, -β, and -γ isoforms), or Wortmannin (a specific PI3′K blocker). The percentage of apoptotic cells is shown on the y-axis. Concentrations of pharmacological inhibitors are shown on the x-axis (μM). Similar results were obtained using different concentrations of p33 peptide or higher concentrations of the inhibitors (not shown). One result representative of five different experiments is shown. (*D* and *E*) Inhibition of p33 peptide–mediated or PMA-mediated apoptosis of P14 TCR Tg $vav^{+/+}$ thymocytes by kinase or actin polymerization blockers. (*D*) Thymocytes were treated with p33 peptide (10^{-9}M) in the absence or presence of RO-31-8220 (*RO*, 1 μM), the actin polymerization blocker CytD (2.5 μM), or Wortmannin (*WT*, 1 μM). (*E*) Thymocytes were treated with PMA (12.5 nM) in the absence or presence of RO-31-8220, CytD, or Wortmannin at the concentrations described for *D*. Unstimulated thymocytes served as controls for both *D* and *E*. Results for *D* and *E* are shown as mean percent viable $CD4^+CD8^+$ cells ± SD. Percentage of apoptosis was determined as described in Materials and Methods. One result representative of three different experiments is shown.

Cooperation between Vav and PKC in Negative Selection. The primary biochemical defects associated with signaling in peptide-specific $vav^{-/-}$ thymocytes were impaired Ca^{2+} flux and reduced actin polymerization. Addition of Ca^{2+} ionophore, which restores Ca^{2+} flux in P14 $vav^{+/-}$ and

vav$^{-/-}$ thymocytes (not shown), did not restore p33 peptide–mediated apoptosis even when used at very high concentrations (100 ng/ml; Fig. 8 *A*). In contrast, activation of *vav*$^{-/-}$ P14 Tg cells with the deleting p33 peptide plus activation of PKC via the phorbol ester PMA significantly shifted the dose–response curve of cell death in a dose-dependent manner (Fig. 8 *B*). Thus, activation of PKC via PMA, but not rescue of Ca^{2+} flux by Ca^{2+} ionophore, was able to restore peptide-specific apoptosis in P14 *vav*$^{-/-}$ thymocytes, suggesting that the Vav and PKC signaling cascades cooperate in the induction of TCR-mediated thymocyte apoptosis. However, it should be noted that our results do not preclude a role for Ca^{2+} elevation in thymocyte selection and clonal deletion in vivo.

Recently, it has been shown that in order for Vav to act as a GDP/GTP exchange factor (GEF) for Rac, RhoA, or CDC42, PI3′K activity and the binding of PI3′K-generated phospholipid products to the PH domain of Vav are required (44). Therefore, we investigated whether the specific PI3′K inhibitor Wortmannin could block peptide-specific apoptosis. As shown in Fig. 8, *C* and *D*, the inhibition of PI3′K did not affect the apoptosis of P14 thymocytes triggered by the deleting p33 peptide, suggesting that the role of Vav in thymocyte apoptosis is independent of PI3′K phospholipid–dependent Vav activation. However, inhibition of PKC by the compound RO-31-8220 (which blocks all PKC isoforms) prevented peptide-specific apoptosis in wild-type thymocytes (Fig. 8, *C* and *D*). Peptide-specific apoptosis of P14 thymocytes was not blocked by the pharmacological inhibitor GF109203X, which prevents activation of Ca^{2+}-dependent PKC isoforms (Fig. 8 *C*). PMA-triggered apoptosis was blocked by the global PKC blocker RO-31-8220 but not by CytD or Wortmannin (Fig. 8 *E*). These data indicate that Vav links TCR signaling to activation of a Ca^{2+}-independent PKC isoform required for the induction of peptide-specific thymocyte apoptosis.

To further evaluate the link between Vav and PKC, we immunoprecipitated Vav from wild-type thymocytes and analyzed the binding of various PKC isoforms to Vav. Surprisingly, Vav coimmunoprecipitated with the Ca^{2+}-independent PKC isoform PKC-θ but not with any other PKC isoform tested (Fig. 9, *left*). The association between Vav and PKC-θ did not change after CD3 cross-linking, suggesting that Vav/PKC-θ binding is constitutive in thymocytes. Constitutive Vav/PKC-θ association was also observed in mature peripheral T cells (not shown). Our results do not preclude associations between Vav and low abundance PKC isoforms.

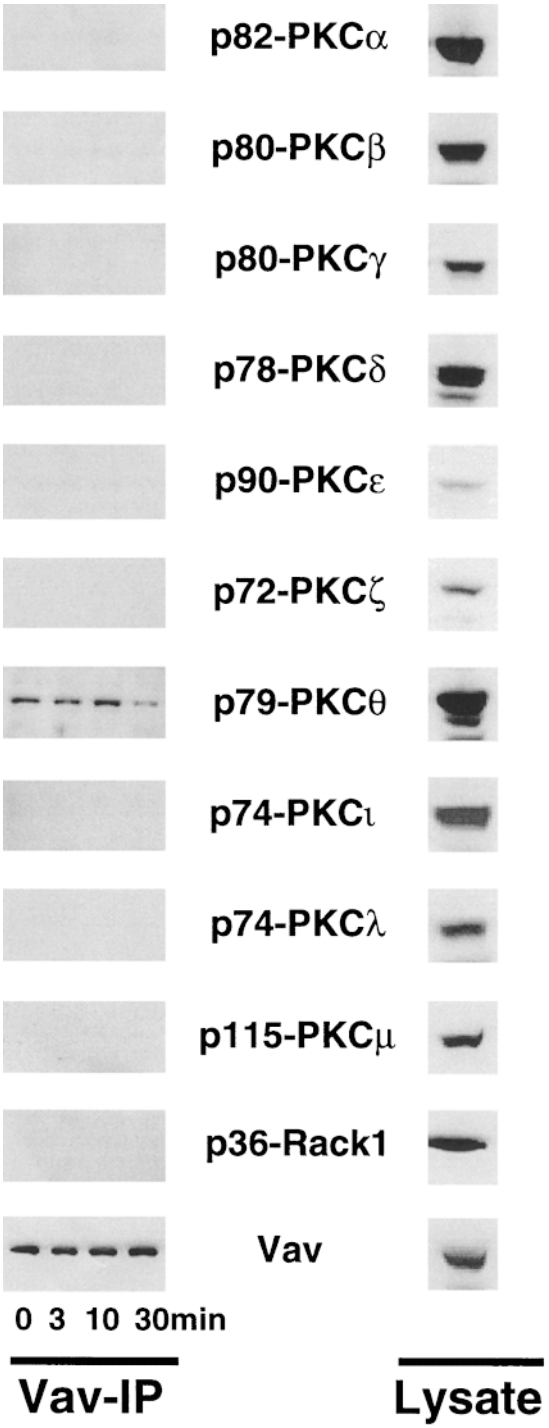

Figure 9. Vav binds constitutively to PKC-θ. Thymocytes (10^7 cells/lane) were activated with anti-CD3ε (1 μg/ml) for the indicated time points. After activation, Vav was immunoprecipitated from lysates and the complexes were Western blotted to detect the presence of different PKC isoforms and Vav (*Vav-IP*; *left*). Right panels (*Lysate*) show the relative protein levels of Vav and different PKC isoforms in total thymocyte lysates (2×10^6 cells/lane). PKC-η and -κ were not tested. The molecular weights of the PKC isoforms are indicated.

Discussion

Our genetic and functional analyses of *vav*$^{-/-}$ mice show that Vav is a crucial regulator both of positive and negative selection of $CD8^+$ thymocytes and the peptide-triggered apoptosis of developing T cells. Vav is involved as a regulator of TCR-mediated cytoskeletal reorganization and Ca^{2+}

mobilization after peptide-specific activation by APCs. Our results suggest that peptide-triggered thymocyte apoptosis is mediated via Vav activation, changes in the actin cytoskeleton, and subsequent activation of a PKC isoform. This hypothesis is based on the following findings: (*a*) Vav-deficient thymocytes do not undergo peptide–MHC-mediated cell death in vitro or in vivo; (*b*) *vav*$^{-/-}$ thymocytes exhibit a defect in actin polymerization, and inhibition of cytoskeletal changes by CytD blocks peptide–MHC-mediated and anti-CD3/anti-CD28–mediated thymocyte apoptosis. However, inhibition of actin polymerization does not inhibit dexamethasone-, CD95-, or PKC-mediated thymocyte apoptosis; (*c*) activation of PKC restores the susceptibility to apoptosis of p33 peptide–triggered P14 Tg *vav*$^{-/-}$ thymocytes, and inhibition of a Ca^{2+}-independent PKC isoform inhibits TCR-mediated thymocyte apoptosis; and (*d*) Vav associates constitutively with PKC-θ but not with any other PKC isoform. Thus, the PKC isoform PKC-θ is a good candidate for the effector kinase of negative thymocyte selection.

The PKCs are a family of 11 phospholipid-dependent serine/threonine kinases. These closely related isoenzymes differ in their structural and biochemical properties, tissue distribution, subcellular localization, and substrate specificity (45, 46). According to primary structure and binding to Ca^{2+} or phorbol esters, different PKC subgroups exist: conventional PKCs (α, βI, βII, and γ) bind Ca^{2+} and are activated by PMA; novel PKCs (δ, ϵ, θ, and η) are activated by PMA but do not bind Ca^{2+}; atypical PKCs (ζ, λ, ι, and μ) bind to diacylglycerol (DAG) but are not activated by PMA or Ca^{2+} ionophores. Activation of PKC molecules by lipid second messengers requires membrane recruitment (47). T cell activation requires PKC activity. Previously, it has been reported using PCR and Northern blotting that PKC-α, -β, -δ, -ϵ, -ζ, and -θ are expressed in thymocytes (48–50). Our study shows for the first time that all PKC isoforms are expressed in thymocytes, albeit at different levels. Although most PKC isoforms are expressed ubiquitously, the isoform PKC-θ is predominantly expressed in the hematopoietic system, particularly in T cells (48–50), and has been placed upstream of IL-2 transactivation and AP1 (Fos/Jun) activity in T lymphoma cells (51, 52). Recently, it has been shown in Jurkat cells that calcineurin and PKC-θ cooperate in inducing IL-2 gene transcription (53), a function that is reminiscent of the coordination of IL-2 expression by calcineurin and Vav/Rac1 (20, 54-57). Interestingly, the small Ras-like molecules Rac1, CDC42, and Rho, whose activation is regulated by Vav, may act upstream of PKC (58, 59), suggesting that Vav, Rac1, and PKC-θ may form a complex. Although Vav and PKC-θ clearly associate in thymocytes and peripheral T cells, Rac1, CDC42, and RhoA do not coimmunoprecipitate with these complexes.

Vav and Vav-regulated Rac1 and CDC42 have been previously shown to mediate changes in the actin cytoskeleton and to activate SAPK/JNK (13–15, 60, 61). Similarly, PKC-θ has been placed upstream of SAPK/JNK in T cell lines (53). However, TCR/CD28-mediated SAPK/JNK activation appears normal in *vav*$^{-/-}$ thymocytes and mature T cells after anti-CD3 cross-linking (19, 20). Similarly, a genetic mutation in the SAPK/JNK signaling pathway had no effect on the induction of thymocyte apoptosis (29), suggesting that Vav and perhaps PKC-θ–mediated negative selection are independent of SAPK/JNK. Importantly, although SAPK/JNK activity is readily induced in thymocytes in response to anti-CD3 and anti-CD28 Abs (62), we failed to detect SAPK/JNK activation in thymocytes after specific peptide–MHC-mediated stimulation. Thus, Vav may define a novel signaling pathway that leads to negative thymocyte selection and IL-2 production in peripheral T cells. This signaling pathway appears to be independent of MAPK, SAPK/JNK, or NF-κB activation.

Rac1, RhoA, or CDC42 activation by Vav requires PI3′K activity in vitro (44). However, inhibition of PI3′K has no apparent effect on the peptide-triggered thymocyte apoptosis of thymocytes, suggesting either that the role of Vav in thymocyte apoptosis is independent of its GTP exchange activity for Rac and CDC42, or that Vav can function as an exchange factor even in the absence of PI3′K activity in vivo. Similarly, it has been shown that a pharmacological PKC inhibitor, but not the PI3′K inhibitor Wortmannin, can block anti-CD3/anti-CD28–mediated thymocyte apoptosis (63). These latter results are consistent with our observation that Vav and PKC regulate anti-CD3/anti-CD28–mediated apoptosis and imply that PKC activation is a crucial signal in the pathway of TCR-triggered apoptosis in developing thymocytes. Whether PKC-θ and/or other PKC isoforms are the crucial downstream kinases in thymocyte selections needs to be determined in genetic experiments.

Both we (19) and Holsinger et al. (20) have previously shown that Vav regulates Ca^{2+} mobilization and actin reorganization in peripheral T cells after anti-CD3ϵ Ab cross-linking. The results of the present study provide the first genetic evidence that Vav is also a crucial regulator of the TCR-mediated Ca^{2+} flux and actin polymerization required for thymocyte selection of peptide–MHC-stimulated thymocytes. In particular, actin polymerization was found to be crucial for the induction of apoptosis. Various cytoskeletal proteins and regulators of cytoskeletal changes, such as gelsolin (64–66), β-catenin (67), PAK2 (68), actin (67, 69–76), fodrin (77), and Gas2 (76), are proteolytically cleaved after the induction of apoptosis. Cleavage of cytoskeletal proteins, which occurs after caspase activation, has an important role in the death effector phase of apoptosis, particularly in the regulation of membrane alterations, morphological changes, and DNA fragmentation (68, 69). In contrast, inhibition of actin polymerization by CytD resulted in impaired TCR-mediated apoptosis. These cytoskeletal changes were found to act upstream of the opening of the mitochondrial membrane pore complex and caspase activation. However, CytD could not block apoptosis after PKC activation (which induces rapid changes in the actin cytoskeleton) and CytD could not protect thymocytes

from dexamethasone- or CD95-mediated apoptosis, suggesting that actin changes per se are not the principle mechanism for conveying a cell death signal in thymocytes. Rather, we propose that TCR-mediated and Vav-regulated changes in the actin cytoskeleton lead to the recruitment and/or assembly of a death effector molecule(s) that relays the TCR signal to the apoptotic machinery.

It has been shown in the D10 T cell line that only PKC-θ translocates to the site of contact between T cells and APCs. All other PKC isoforms (α, β1, δ, η, and ζ) are excluded from the contact site, suggesting that PKC-θ has a specific role in T cell activation (78). Since Vav regulates TCR clustering and PKC-θ is found in these clusters, Vav-regulated actin polymerization may be required for recruitment of PKC-θ to the TCR and activation of PKC at the cell membrane. How Vav and possibly PKC-θ link TCR-mediated signals to mitochondrial apoptosis and caspase 3 activation remains to be determined. Importantly, our results show that Vav and actin polymerization also regulate the extent and duration of peptide-specific Ca^{2+} mobilization, an event thought to be involved in thymocyte apoptosis and clonal selection (79–83).

Our data show that Vav regulates positive and negative selection of MHC class I–restricted thymocytes. We have previously reported that the progression of $CD4^-CD8^-$ T cell precursor cells to $CD4^+CD8^+$ thymocytes is impaired in *vav*$^{-/-}$ mice on a C57BL/6 (H-$2^{b/b}$) background but not on a CD1 (H-$2^{q/q}$) background (19). Thus, Vav clearly has a role in preTCR-mediated expansion of early thymocytes, but the absence of Vav can be partially compensated by other signaling molecules. However, this compensatory mechanism does not appear to be operational or sufficient to rescue positive and negative selection of TCR Tg thymocytes in *vav*$^{-/-}$ mice. Thus, Vav either plays a different role in TCR signaling at different stages of development and/or different compensatory mechanisms are available to $CD4^-CD8^-$ versus $CD4^+CD8^+$ thymocytes that make up for the Vav mutation in the expansion from $CD4^-CD8^-$ to $CD4^+CD8^+$ cells but cannot compensate for selection of $CD4^+CD8^+$ thymocytes.

Conclusion. Our data provide the first genetic evidence for a role for Vav in peptide–MHC-triggered cytoskeletal reorganization in vivo. These results indicate that Vav-regulated actin reorganization is a crucial prerequisite for antigen receptor–mediated selection and apoptosis in peptide-specific thymocytes. We have shown that Vav and the actin cytoskeleton regulate the extent and duration of Ca^{2+} mobilization after peptide-specific activation, and that Vav functions upstream of mitochondrial pore opening and caspase activation. The defect in peptide-specific apoptosis in *vav*$^{-/-}$ thymocytes can be overcome by activation of PKC, and the inhibition of PKC blocks peptide-specific cell death in wild-type thymocytes, indicating that PKC activation is the trigger for thymocyte apoptosis in response to peptide. Of all PKC isoforms tested, Vav associated only with the PKC-θ isoform expressed primarily in T cells, suggesting that PKC-θ is the crucial kinase involved in thymocyte selection and clonal deletion.

We thank K. Bachmaier, K. Tedford, A. Oliveira-dos-Santos, T. Sasaki, H. Nishina, A. Tafuri-Bladt, and L. Zhang for helpful comments, and M. Saunders for scientific editing.

This work was supported by grants from the Medical Research Council of Canada (to J.M. Penninger and A. Bernstein); from the National Cancer Institute of Canada (to A. Bernstein); and from the Deutsche Forschungsgemeinschaft (SFB 465; to K.-D. Fischer).

Address correspondence to Josef M. Penninger, The Amgen Institute, Ontario Cancer Institute, Departments of Medical Biophysics and Immunology, University of Toronto, 620 University Ave., Toronto, Ontario M5G 2C1, Canada. Phone: 416-204-2241; Fax: 416-204-2278; E-mail: jpenning@amgen.com

Received for publication 7 July 1998 and in revised form 10 September 1998.

References

1. Collins, T.L., M. Deckert, and A. Altman. 1997. Views on Vav. *Immunol. Today*. 18:221–225.
2. Bustelo, X.R., J.A. Ledbetter, and M. Barbacid. 1992. Product of vav proto-oncogene defines a new class of tyrosine protein kinase substrates. *Nature*. 356:68–71.
3. Margolis, B., P. Hu, S. Katzav, W. Li, J.M. Oliver, A. Ullrich, A. Weiss, and J. Schlessinger. 1992. Tyrosine phosphorylation of vav proto-oncogene product containing SH2 domain and transcription factor motifs. *Nature*. 356:71–74.
4. Katzav, S., D. Martin-Zanca, and M. Barbacid. 1989. vav, a novel human oncogene derived from a locus ubiquitously expressed in hematopoietic cells. *EMBO J.* 8:2283–2290.
5. Teramoto, H., P. Crespo, O.A. Coso, T. Igishi, N.Z. Xu, and J.S. Gutkind. 1996. The small GTP-binding protein rho activates c-Jun N-terminal kinases/stress-activated protein kinases in human kidney 293T cells. Evidence for a Pak-independent signaling pathway. *J. Biol. Chem*. 271:25731–25734.
6. Coso, O.A., M. Chiariello, G. Kalinec, J.M. Kyriakis, J. Woodgett, and J.S. Gutkind. 1995. Transforming G protein-coupled receptors potently activate JNK (SAPK). Evidence for a divergence from the tyrosine kinase signaling pathway. *J. Biol. Chem*. 270:5620–5624.
7. Tapon, N., and A. Hall. 1997. Rho, Rac and Cdc42 GTPases regulate the organization of the actin cytoskeleton.

Curr. Opin. Cell Biol. 9:86–92.
8. Minden, A., A. Lin, F.X. Claret, A. Abo, and M. Karin. 1995. Selective activation of the JNK signaling cascade and c-Jun transcriptional activity by the small GTPases Rac and Cdc42Hs. *Cell.* 81:1147–1157.
9. Knaus, U.G., S. Morris, H.J. Dong, J. Chernoff, and G.M. Bokoch. 1995. Regulation of human leukocyte p21-activated kinases through G protein–coupled receptors. *Science.* 269:221–223.
10. Sells, M.A., U.G. Knaus, S. Bagrodia, D.M. Ambrose, G.M. Bokoch, and J. Chernoff. 1997. Human p21-activated kinase (Pak1) regulates actin organization in mammalian cells. *Curr. Biol.* 7:202–210.
11. Gulbins, E., K.M. Coggeshall, C. Langlet, G. Baier, N. Bonnefoyberard, P. Burn, A. Wittinghofer, S. Katzav, and A. Altman. 1994. Activation of Ras in vitro and in intact fibroblasts by the Vav guanine nucleotide exchange protein. *Mol. Cell. Biol.* 14:906–913.
12. Gulbins, E., K.M. Coggeshall, G. Baier, S. Katzav, P. Burn, and A. Altman. 1993. Tyrosine kinase-stimulated guanine nucleotide exchange activity of Vav in T cell activation. *Science.* 260:822–825.
13. Crespo, P., K.E. Schuebel, A.A. Ostrom, J.S. Gutkind, and X.R. Bustelo. 1997. Phosphotyrosine-dependent activation of Rac-1 GDP/GTP exchange by the vav proto-oncogene product. *Nature.* 385:169–172.
14. Crespo, P., X.R. Bustelo, D.S. Aaronson, O.A. Coso, M. Lopez-Barahona, M. Barbacid, and J.S. Gutkind. 1996. Rac-1 dependent stimulation of the Jnk/Sapk signaling pathway by Vav. *Oncogene.* 13:455–460.
15. Han, J.W., B. Das, W. Wei, L. Van Aelst, R.D. Mosteller, R. Khosravi-Far, J.K. Westwick, C.J. Der, and D. Broek. 1997. Lck regulates Vav activation of members of the Rho family of GTPases. *Mol. Cell. Biol.* 17:1346–1353.
16. Fischer, K.D., A. Zmuldzinas, S. Gardner, M. Barbacid, A. Bernstein, and C. Guidos. 1995. Defective T-cell receptor signalling and positive selection of Vav-deficient CD4+ CD8+ thymocytes. *Nature.* 374:474–477.
17. Tarakhovsky, A., M. Turner, S. Schaal, P.J. Mee, L.P. Duddy, K. Rajewsky, and V.L. Tybulewicz. 1995. Defective antigen receptor-mediated proliferation of B and T cells in the absence of Vav. *Nature.* 374:467–470.
18. Zhang, R., F.W. Alt, L. Davidson, S.H. Orkin, and W. Swat. 1995. Defective signalling through the T- and B-cell antigen receptors in lymphoid cells lacking the vav proto-oncogene. *Nature.* 374:470–473.
19. Fischer, K.D., Y.Y. Kong, H. Nishina, K. Tedford, L.E.M. Marengere, I. Kozieradzki, T. Sasaki, M. Starr, G. Chan, S. Gardener, et al. 1998. Vav is a regulator of cytoskeletal reorganization mediated by the T-cell receptor. *Curr. Biol.* 8:554–562.
20. Holsinger, L.J., I.A. Graef, W. Swat, T. Chi, D.M. Bautista, L. Davidson, R.S. Lewis, F.W. Alt, and G.R. Crabtree. 1998. Defects in actin-cap formation in Vav-deficient mice implicate an actin requirement for lymphocyte signal transduction. *Curr. Biol.* 8:563–572.
21. Turner, M., P.J. Mee, A.E. Walters, M.E. Quinn, A.L. Mellor, R. Zamoyska, and V.L.J. Tybulewicz. 1997. A requirement for the Rho-family GTP exchange factor Vav in positive and negative selection of thymocytes. *Immunity.* 7:451–460.
22. Teh, H.S., P. Kisielow, B. Scott, H. Kishi, Y. Uematsu, H. Bluethmann, and H. von Boehmer. 1988. Thymic major histocompatibility complex antigens and the alpha beta T-cell receptor determine the CD4/CD8 phenotype of T cells. *Nature.* 335:229–233.
23. Pircher, H., T.W. Mak, R. Lang, W. Ballhausen, E. Rueedi, H. Hengartner, R.M. Zinkernagel, and K. Buerki. 1989. T cell tolerance to Mlsa encoded antigens in T cell receptor V beta 8.1 chain transgenic mice. *EMBO J.* 8:719–727.
24. von Boehmer, H., H.S. Teh, and P. Kisielow. 1989. The thymus selects the useful, neglects the useless and destroys the harmful. *Immunol. Today.* 10:57–61.
25. Kisielow, P., H.S. Teh, H. Bluethmann, and H. von Boehmer. 1988. Positive selection of antigen-specific T cells in thymus by restricting MHC molecules. *Nature.* 335:730–733.
26. Sebzda, E., V.A. Wallace, J. Mayer, R.S. Yeung, T.W. Mak, and P.S. Ohashi. 1994. Positive and negative thymocyte selection induced by different concentrations of a single peptide. *Science.* 263:1615–1618.
27. Sebzda, E., T.M. Kuendig, C.T. Thomson, K. Aoki, S.Y. Mak, J.P. Mayer, T. Zamborelli, S.G. Nathenson, and P.S. Ohashi. 1996. Mature T cell reactivity altered by peptide agonist that induces positive selection. *J. Exp. Med.* 183:1093–1104.
28. Harris, W., S.E. Wilkinson, and J.S. Nixon. 1997. Recent developments in protein kinase C inhibitors. *Expert Opin. Ther. Patents.* 7:63–68.
29. Nishina, H., K.D. Fischer, L. Radvanyi, A. Shahinian, R. Hakem, E.A. Rubie, A. Bernstein, T.W. Mak, J.R. Woodgett, and J.M. Penninger. 1997. Stress-signalling kinase Sek1 protects thymocytes from apoptosis mediated by CD95 and CD3. *Nature.* 385:350–353.
30. Pircher, H., K. Brduscha, U. Steinhoff, M. Kasai, T. Mizuochi, R.M. Zinkernagel, H. Hengartner, B. Kyewski, and K.P. Mueller. 1993. Tolerance induction by clonal deletion of CD4+8+ thymocytes in vitro does not require dedicated antigen-presenting cells. *Eur. J. Immunol.* 23:669–674.
31. Schmid, I., C.H. Uittenbogaart, and J.V. Giorgi. 1994. Sensitive method for measuring apoptosis and cell surface phenotype in human thymocytes by flow cytometry. *Cytometry.* 15: 12–20.
32. Susin, S.A., N. Zamzami, M. Castedo, T. Hirsch, P. Marchetti, A. Macho, E. Daugas, M. Geuskens, and G. Kroemer. 1996. Bcl-2 inhibits the mitochondrial release of an apoptogenic protease. *J. Exp. Med.* 184:1331–1341.
33. Zamzami, N., S.A. Susin, P. Marchetti, T. Hirsch, M.-I. Gomez, M. Castedo, and K. Guido. 1996. Mitochondrial control of nuclear apoptosis. *J. Exp. Med.* 183:1533–1544.
34. Baeuerle, P.A., and D. Baltimore. 1996. NF-kappa B: ten years after. *Cell.* 87:13–20.
35. Valitutti, S., M. Dessing, K. Aktories, H. Gallati, and A. Lanzavecchia. 1995. Sustained signaling leading to T cell activation results from prolonged T cell receptor occupancy. Role of T cell actin cytoskeleton. *J. Exp. Med.* 181:577–584.
36. Penninger, J.M., and G. Kroemer. 1998. Molecular and cellular mechanisms of T lymphocyte apoptosis. *Adv. Immunol.* 68:51–144.
37. Punt, J.A., B.A. Osborne, Y. Takahama, S.O. Sharrow, and A. Singer. 1994. Negative selection of $CD4^+CD8^+$ thymocytes by T cell receptor–induced apoptosis requires a costimulatory signal that can be provided by CD28. *J. Exp. Med.* 179:709–713.
38. Zamzami, N., P. Marchetti, M. Castedo, D. Decaudin, A. Macho, T. Hirsch, S.A. Susin, P.X. Petit, B. Mignotte, and G. Kroemer. 1995. Sequential reduction of mitochondrial transmembrane potential and generation of reactive oxygen

species in early programmed cell death. *J. Exp. Med.* 182: 367–377.
39. Yang, J., X. Liu, K. Bhalla, C.N. Kim, A.M. Ibrado, J. Cai, T.I. Peng, D.P. Jones, and X. Wang. 1997. Prevention of apoptosis by Bcl-2: release of cytochrome c from mitochondria blocked. *Science.* 275:1129–1132.
40. Liu, X., C.N. Kim, J. Yang, R. Jemmerson, and X. Wang. 1996. Induction of apoptotic program in cell-free extracts: requirement for dATP and cytochrome c. *Cell.* 86:147–157.
41. Kluck, R.M., W.-E. Bossy, D.R. Green, and D.D. Newmeyer. 1997. The release of cytochrome c from mitochondria: a primary site for Bcl-2 regulation of apoptosis. *Science.* 275:1132–1136.
42. Alam, A., M.Y. Braun, F. Hartgers, S. Lesage, L. Cohen, P. Hugo, F. Denis, and R.P. Sekaly. 1997. Specific activation of the cysteine protease CPP32 during the negative selection of T cells in the thymus. *J. Exp. Med.* 186:1503–1512.
43. Jameson, S.C., K.A. Hogquist, and M.J. Bevan. 1995. Positive selection of thymocytes. *Annu. Rev. Immunol.* 13:93–126.
44. Han, J.W., K. Luby-Phelps, B. Das, X.D. Shu, Y. Xia, R.D. Mosteller, U.M. Krishna, J.R. Falck, M.A. White, and D. Broek. 1998. Role of substrates and products of PI 3-kinase in regulating activation of Rac-related guanosine triphosphatases by Vav. *Science.* 279:558–560.
45. Hofmann, J. 1997. The potential for isoenzyme-selective modulation of protein kinase C. *FASEB J.* 11:649–669.
46. Baron-Delage, S., and G. Cherqui. 1997. Protein kinase C and tumorigenic potential. *Bull. Cancer.* 84:829–832.
47. Mochly-Rosen, D., and A.S. Gordon. 1998. Anchoring proteins for protein kinase C: a means for isozyme selectivity. *FASEB J.* 12:35–42.
48. Baier, G., B.-G. Baier, N. Meller, K.M. Coggeshall, L. Giampa, D. Telford, N. Isakov, and A. Altman. 1994. Expression and biochemical characterization of human protein kinase C-theta. *Eur. J. Biochem.* 225:195–203.
49. Mischak, H., J. Goodnight, D.W. Henderson, S. Osada, S. Ohno, and J.F. Mushinski. 1993. Unique expression pattern of protein kinase C-theta: high mRNA levels in normal mouse testes and in T-lymphocytic cells and neoplasms. *FEBS Lett.* 326:51–55.
50. Chang, J.D., Y. Xu, M.K. Raychowdhury, and J.A. Ware. 1993. Molecular cloning and expression of a cDNA encoding a novel isoenzyme of protein kinase C (nPKC). A new member of the nPKC family expressed in skeletal muscle, megakaryoblastic cells, and platelets. *J. Biol. Chem.* 268:14208–14214.
51. Szamel, M., A. Appel, R. Schwinzer, and K. Resch. 1998. Different protein kinase C isoenzymes regulate IL-2 receptor expression or IL-2 synthesis in human lymphocytes stimulated via the TCR. *J. Immunol.* 160:2207–2214.
52. Baier, B.-G., F. Uberall, B. Bauer, F. Fresser, H. Wachter, H. Grunicke, G. Utermann, A. Altman, and G. Baier. 1996. Protein kinase C-theta isoenzyme selective stimulation of the transcription factor complex AP-1 in T lymphocytes. *Mol. Cell. Biol.* 16:1842–1850.
53. Werlen, G., E. Jacinto, Y. Xia, and M. Karin. 1998. Calcineurin preferentially synergizes with PKC-theta to activate JNK and IL-2 promoter in T lymphocytes. *EMBO J.* 17: 3101–3111.
54. Raab, M., A.J. da Silva, P.R. Findell, and C.E. Rudd. 1997. Regulation of Vav-SLP-76 binding by ZAP-70 and its relevance to TCR zeta/CD3 induction of interleukin-2. *Immunity.* 6:155–164.
55. Tuosto, L., F. Michel, and O. Acuto. 1996. p95vav associates with tyrosine-phosphorylated SLP-76 in antigen-stimulated T cells. *J. Exp. Med.* 184:1161–1166.
56. Wu, J., D.G. Motto, G.A. Koretzky, and A. Weiss. 1996. Vav and SLP-76 interact and functionally cooperate in IL-2 gene activation. *Immunity.* 4:593–602.
57. Jacinto, E., G. Werlen, and M. Karin. 1998. Cooperation between Syk and Rac1 leads to synergistic JNK activation in T lymphocytes. *Immunity.* 8:31–41.
58. Cantrell, D. 1996. T cell antigen receptor signal transduction pathways. *Annu. Rev. Immunol.* 14:259–274.
59. Arnould, T., E. Kim, L. Tsiokas, F. Jochimsen, W. Gruning, J.D. Chang, and G. Walz. 1998. The polycystic kidney disease 1 gene product mediates protein kinase C alpha-dependent and c-Jun N-terminal kinase-dependent activation of the transcription factor AP-1. *J. Biol. Chem.* 273:6013–6018.
60. Khosravi, F.-R., W.-M. Chrzanowska, P.A. Solski, A. Eva, K. Burridge, and C.J. Der. 1994. Dbl and Vav mediate transformation via mitogen-activated protein kinase pathways that are distinct from those activated by oncogenic Ras. *Mol. Cell. Biol.* 14:6848–6857.
61. Olson, M.F., N.G. Pasteris, J.L. Gorski, and A. Hall. 1996. Faciogenital dysplasia protein (FGD1) and Vav, two related proteins required for normal embryonic development, are upstream regulators of Rho GTPases. *Curr. Biol.* 6:1628–1633.
62. Nishina, H., M. Bachmann, A.J. Oliveira-dos-Santos, I. Kozieradzki, K.D. Fischer, B. Odermatt, A. Wakeham, A. Shahinian, H. Takimoto, A. Bernstein, et al. 1997. Impaired CD28-mediated interleukin 2 production and proliferation in stress kinase SAPK/ERK1 kinase (SEK1)/mitogen-activated protein kinase kinase 4 (MKK4)-deficient T lymphocytes. *J. Exp. Med.* 186:941–953.
63. Punt, J.A., W. Havran, R. Abe, A. Sarin, and A. Singer. 1997. T cell receptor (TCR)-induced death of immature $CD4^+CD8^+$ thymocytes by two distinct mechanisms differing in their requirement for CD28 costimulation: implications for negative selection in the thymus. *J. Exp. Med.* 186: 1911–1922.
64. Kothakota, S., T. Azuma, C. Reinhard, A. Klippel, J. Tang, K.T. Chu, T.J. McGarry, M.W. Kirschner, K. Koths, D.J. Kwiatkowski, and L.T. Williams. 1997. Caspase-3-generated fragment of gelsolin: effector of morphological change in apoptosis. *Science.* 278:294–298.
65. Ohtsu, M., N. Sakai, H. Fujita, M. Kashiwagi, S. Gasa, S. Shimizu, Y. Eguchi, Y. Tsujimoto, Y. Sakiyama, K. Kobayashi, and N. Kuzumaki. 1997. Inhibition of apoptosis by the actin-regulatory protein gelsolin. *EMBO J.* 16:4650–4656.
66. Davoodian, K., B.W. Ritchings, R. Ramphal, and M.R. Bubb. 1997. Gelsolin activates DNase I in vitro and in cystic fibrosis sputum. *Biochemistry.* 36:9637–9641.
67. Brancolini, C., D. Lazarevic, J. Rodriguez, and C. Schneider. 1997. Dismantling cell-cell contacts during apoptosis is coupled to a caspase-dependent proteolytic cleavage of beta-catenin. *J. Cell Biol.* 139:759–771.
68. Rudel, T., and G.M. Bokoch. 1997. Membrane and morphological changes in apoptotic cells regulated by caspase-mediated activation of PAK2. *Science.* 276:1571–1574.
69. Villa, P.G., W.J. Henzel, M. Sensenbrenner, C.E. Henderson, and B. Pettmann. 1998. Calpain inhibitors, but not caspase inhibitors, prevent actin proteolysis and DNA fragmentation during apoptosis. *J. Cell Sci.* 111:713–722.
70. Yang, F.S., X.Y. Sun, W. Beech, B. Teter, S. Wu, J. Sigel,

H.V. Vinters, S.A. Frautschy, and G.M. Cole. 1998. Antibody to caspase-cleaved actin detects apoptosis in differentiated neuroblastoma and plaque-associated neurons and microglia in Alzheimer's disease. *Am. J. Pathol*. 152:379–389.

71. Sakahira, H., M. Enari, and S. Nagata. 1998. Cleavage of CAD inhibitor in CAD activation and DNA degradation during apoptosis. *Nature*. 391:96–99.
72. Donovan, F.M., C.J. Pike, C.W. Cotman, and D.D. Cunningham. 1997. Thrombin induces apoptosis in cultured neurons and astrocytes via a pathway requiring tyrosine kinase and RhoA activities. *J. Neurosci*. 17:5316–5326.
73. Brown, S.B., K. Bailey, and J. Savill. 1997. Actin is cleaved during constitutive apoptosis. *Biochem. J*. 323:233–237.
74. Mashima, T., M. Naito, K. Noguchi, D.K. Miller, D.W. Nicholson, and T. Tsuruo. 1997. Actin cleavage by CPP-32/apopain during the development of apoptosis. *Oncogene*. 14: 1007–1012.
75. Kayalar, C., T. Ord, M.P. Testa, L.T. Zhong, and D.E. Bredesen. 1996. Cleavage of actin by interleukin 1 beta-converting enzyme to reverse DNase I inhibition. *Proc. Natl. Acad. Sci. USA*. 93:2234–2238.
76. Brancolini, C., M. Benedetti, and C. Schneider. 1995. Microfilament reorganization during apoptosis: the role of Gas2, a possible substrate for ICE-like proteases. *EMBO J.* 14: 5179–5190.
77. Martin, S.J., G.A. O'Brien, W.K. Nishioka, A.J. McGahon, A. Mahboubi, T.C. Saido, and D.R. Green. 1995. Proteolysis of fodrin (non-erythroid spectrin) during apoptosis. *J. Biol. Chem.* 270:6425–6428.
78. Monks, C.R., H. Kupfer, I. Tamir, A. Barlow, and A. Kupfer. 1997. Selective modulation of protein kinase C-theta during T-cell activation. *Nature*. 385:83–86.
79. Vasquez, N.J., L.P. Kane, and S.M. Hedrick. 1994. Intracellular signals that mediate thymic negative selection. *Immunity*. 1:45–56.
80. Nakayama, T., Y. Ueda, H. Yamada, E.W. Shores, A. Singer, and C.H. June. 1992. In vivo calcium elevations in thymocytes with T cell receptors that are specific for self ligands. *Science*. 257:96–99.
81. Khan, A.A., M.J. Soloski, A.H. Sharp, G. Schilling, D.M. Sabatini, S.H. Li, C.A. Ross, and S.H. Snyder. 1996. Lymphocyte apoptosis: mediation by increased type 3 inositol 1,4,5-trisphosphate receptor. *Science*. 273:503–507.
82. Jayaraman, T., and A.R. Marks. 1997. Cells deficient in the inositol 1,4,5-trisphosphate receptor are resistant to apoptosis. *Mol. Cell. Biol*. 17:3005–3012.
83. McConkey, D.J., P. Hartzell, P.-J.F. Amador, S. Orrenius, and M. Jondal. 1989. Calcium-dependent killing of immature thymocytes by stimulation via the CD3/T cell receptor complex. *J. Immunol*. 143:1801–1806.